الجامعة الإسلامية العالمية ماليزيا
INTERNATIONAL ISLAMIC UNIVERSITY MALAYSIA

AUTONOMOUS SYSTEMS & ROBOTICS RESEARCH UNIT

AUTONOMOUS SYSTEMS AND ROBOTICS RESEARCH UNIT

# Harnessing Bio-signals for Advanced Man-Machine Applications

**Shahrul Naim Sidek**
*Dept. of Mechatronics Engineering, IIUM*

***International Conference on Innovative Technology, Engineering and Sciences*** *(iCITES'18),*
*UNIMAP, PEKAN, PAHANG*
*1 March 2018*

 

# Outline

1. Fundamental and historical background of bio-signals
2. Research 1: Muscle modeling from biosignals
3. Research 2: Emotion identification from biosignals

# Introduction

1. Bio-signals are widely used for assessment of human functional states

2. Use in classical application in medical diagnosis to consumer products with emotion detection

# Definition

Within the scope of biomedical signals and sensors – biosignal is a description of a physiological phenomenon in living beings

In the broadest sense, the variety of biosignals extends from visual inspection of a patient ..

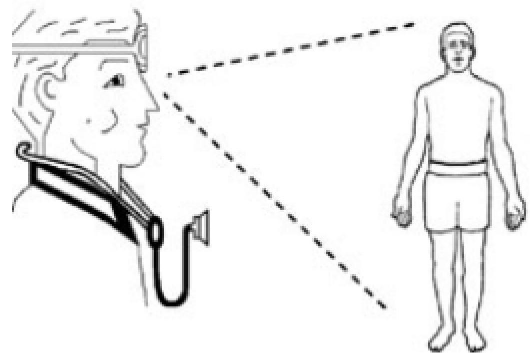

*

.. up to signals recorded from human body by the mean of sensors

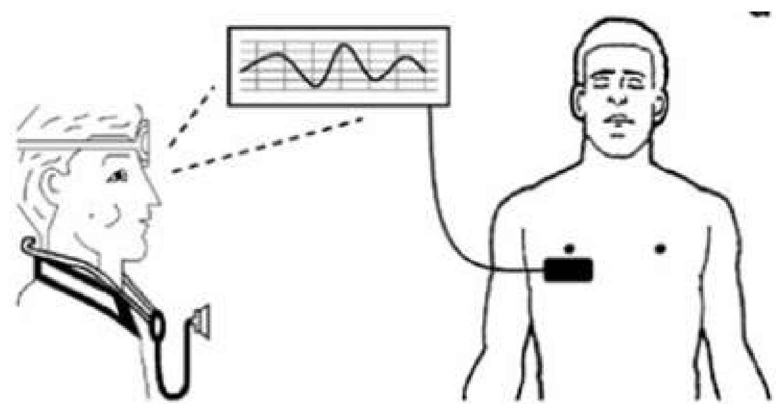

*

# Amongst the very first biosignals

… for diagnostic purpose using different methods

**Inspection** : visualization by the use of naked eye

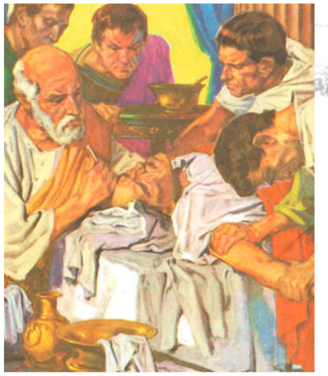

Hippocrates of Cos (c. 460 – c. 375 BC) – "It is necessary to begin with the most important things and those most easily recognized."*

**Palpation** : feeling of body surface, often accompanied by soft pressure

Galen of Pergamum (129-200) – "The feeling of artery striking the fingers" when describing pulsation – "the worm –like pulse, feeble and beating quickly, the ant-like pulse that has sunk to extreme limit of feebleness"

# Amongst the very first biosignals

… for diagnostic purpose using different methods

**Percussion** : striking the body with short, sharp taps of a finger

Leopold Auenbrugger (1722-1809) – introduced the technique - "a slow tapping with the fingers, brought closed together and extended, on the finger of the other hand laid on the chest".

**Auscultation** : listening inner body sounds

Rene T. H. Laennec (1781-1826) –invented the precursor to modern stethoscope from a roll of paper applied to precordial region at one end and his ear at the other end 1816

# Problem with original bio-signals acquisition methods

Lack objective evaluation of diagnosis:

<u>Proof of biosignals</u> – the signal couldn't be reproduced due to observer's variability and lack of archival storage

<u>Analysis of biosignals</u> – really relied on the physician instantaneous impression , thus strongly restricted to personal experience

# Problem with original bio-sisgnal acquisition methods

Lack objective evaluation of diagnosis:

Comparison of biosignals – also depend on the physician and one's experience

Dissemination of biosignals – lack of archives

# Notable contemporary solutions to the problems

Produce objective characterization:

Verbal description – Ibn Sina (980-1037), defined 50 different pulses – “irregular pulse as the flight of a gazelle; stonebullet shot out of a crossbow; scattered leaves”.

Musical note – Francois Nicolas Marquet (1687-1759), defined 30 different pulses documented in musical notes.

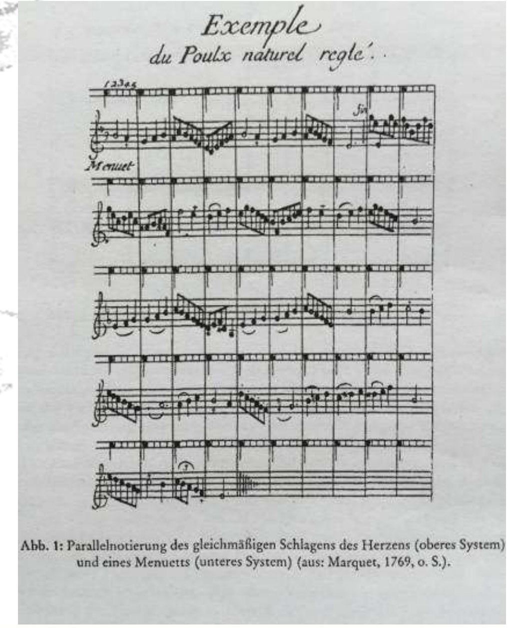

Abb. 1: Parallelnotierung des gleichmäßigen Schlagens des Herzens (oberes System) und eines Menuetts (unteres System) (aus: Marquet, 1769, o. S.).

# Notable contemporary solution to the problems

## Objective characterization

Technical tool – In 1855, Karl von Vierordt (1818-1884) invented the first sphygmograph to measure blood pressure using mechanical balance and weight.

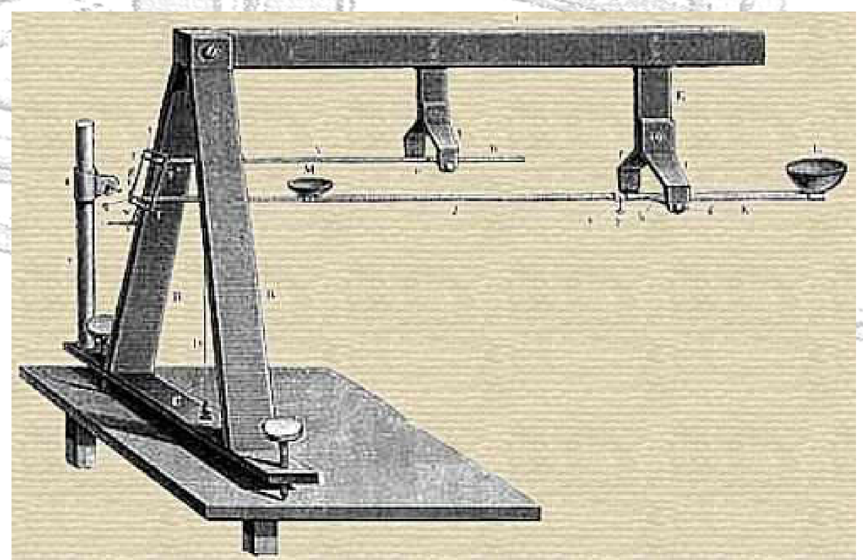

# Classification of biosignals

Based on the origin of the signals:

- -Electrical
- -Magnetic
- -Mechanic
- -Optic
- -Acoustic
- -Chemical
- -Thermal
- -Others

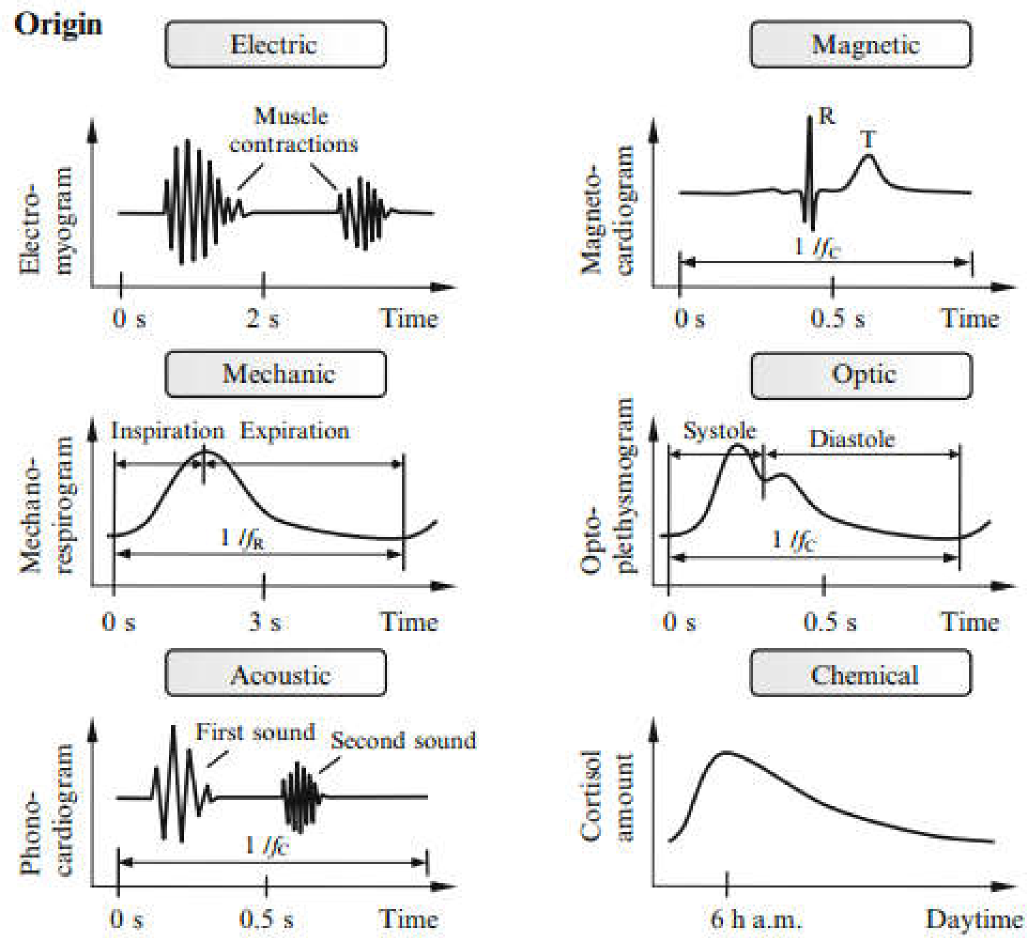

# Trend in biosignals monitoring and applications

Biosignals reflect human health and well-being

The development in the field is fast.

From pre-screening of human functional state and diagnosis of illness,

- it has moved on to subsequent therapy, follow-up treatment, appraisal of it efficiency
- it has improved the quality of interaction between the man and the machine

# Research in BioMechatronics Laboratory, IIUM

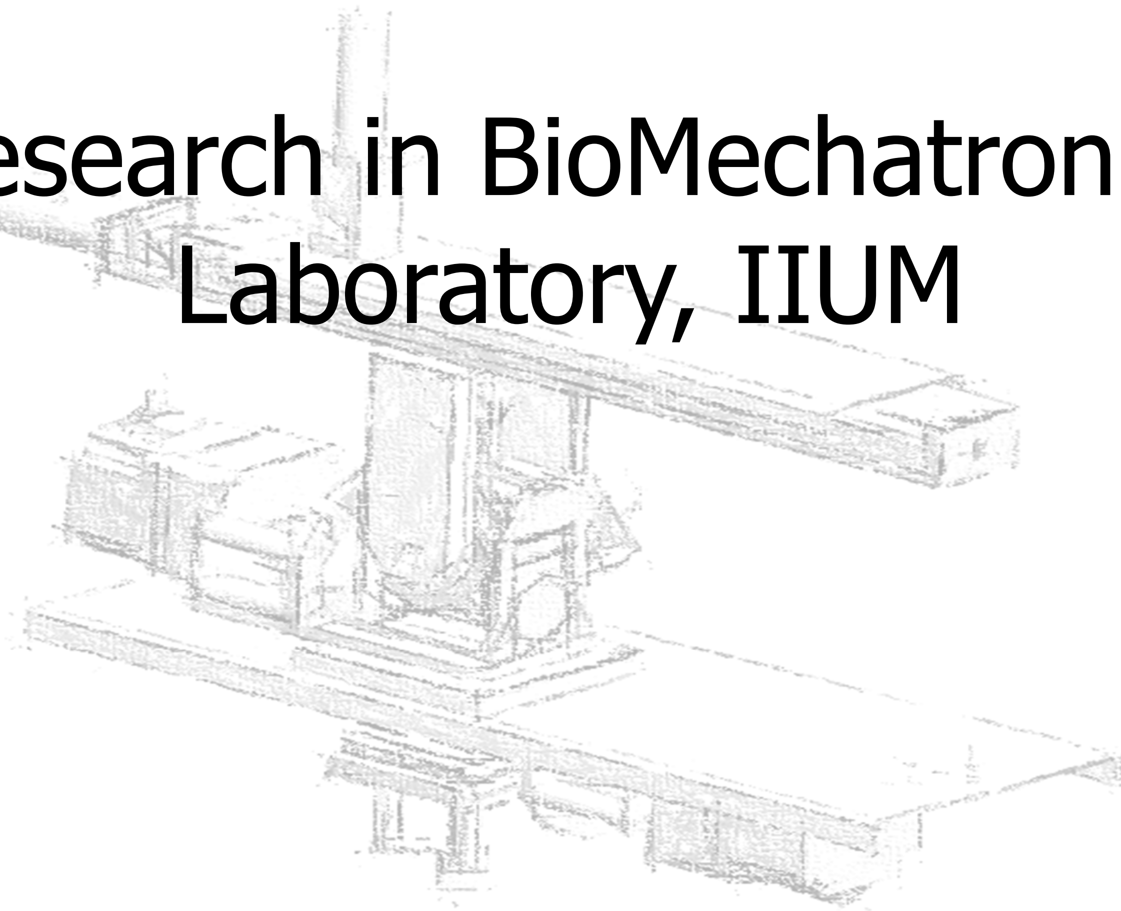

# 1. Hill’s muscle model to predict thumb tip force

Traumatic injury on thumb, the only opposable digit could great affect the function of hand.

In case of total amputation, the muscles in remaining part however still function in normal way.

Motivation is to leverage muscle information to develop prosthetics/orthotics devices that could perform as close as  the original thumb.

# 1. Hill's muscle model to predict thumb tip force

Objective: To develop thumb tip force prediction model using biosignals : **EMG** & **Ultrasound signal of muscle lengths**

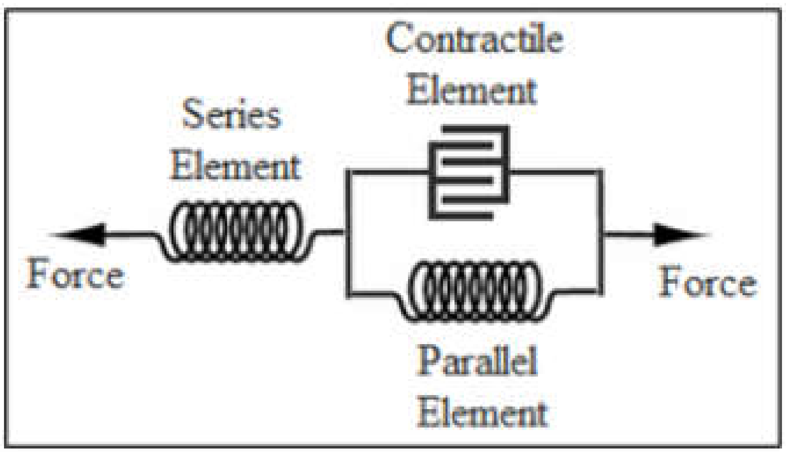


Figure: General Hill's muscle model

# 1. Hill's muscle model to predict thumb tip force

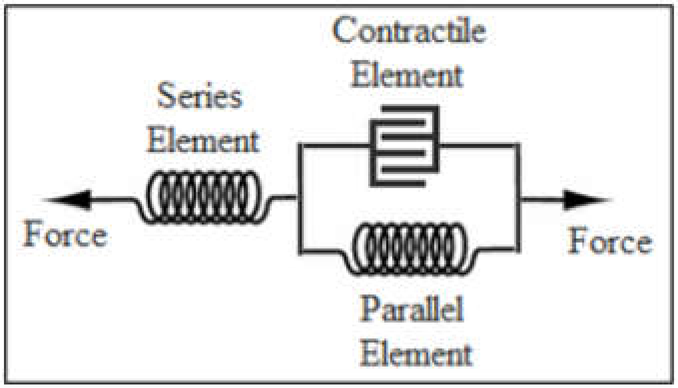


Figure: General Hill's muscle model

$$F_{muscle} = F_{CE} + F_{PE}$$

$$F_{CE} = a \cdot f_1 \cdot F_{CE_{max}}$$

- Represent force from the action of fibrous protein; actin and myosin.

$$F_{PE} = \left(\frac{F_{PE_{max}}}{e^S - 1}\right) \cdot \left(e^{\left(\left(\frac{S}{\Delta L_{PE_{max}}}\right)\Delta L_{PE}\right)} - 1\right)$$

- Represent force resulted from the refusal of the muscle to contract

Using PSO to identify unknown constants

# 1. Hill's muscle model to predict thumb tip force – thumb muscles

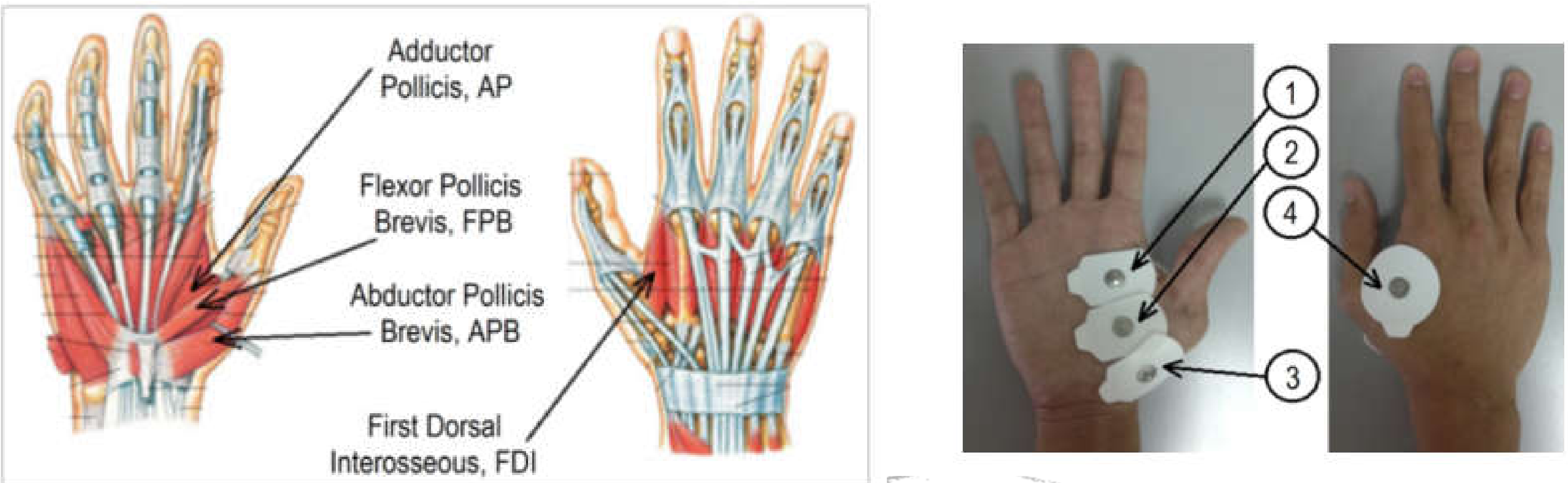


Figure: Thumb intrinsic muscles governing thumb flexion ROM

# 1. Hill’s muscle model to predict thumb tip force – measurement system

Videoclip: System operation

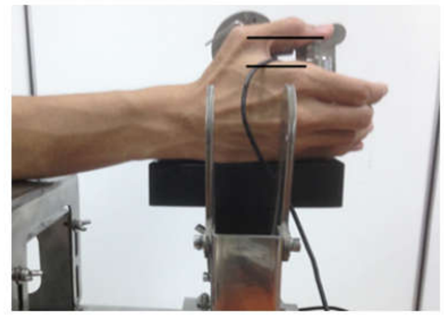

Figure: Thumb flexion at 0 degree

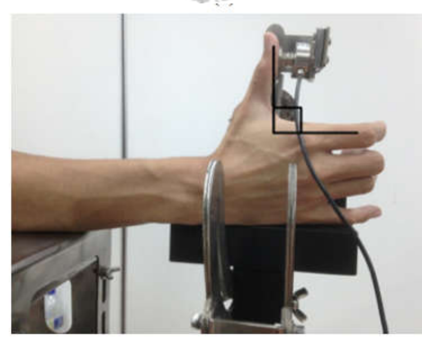

Figure: Thumb flexion at 90 degree

# 1. Hill's muscle model to predict thumb tip force – EMG using Gtec

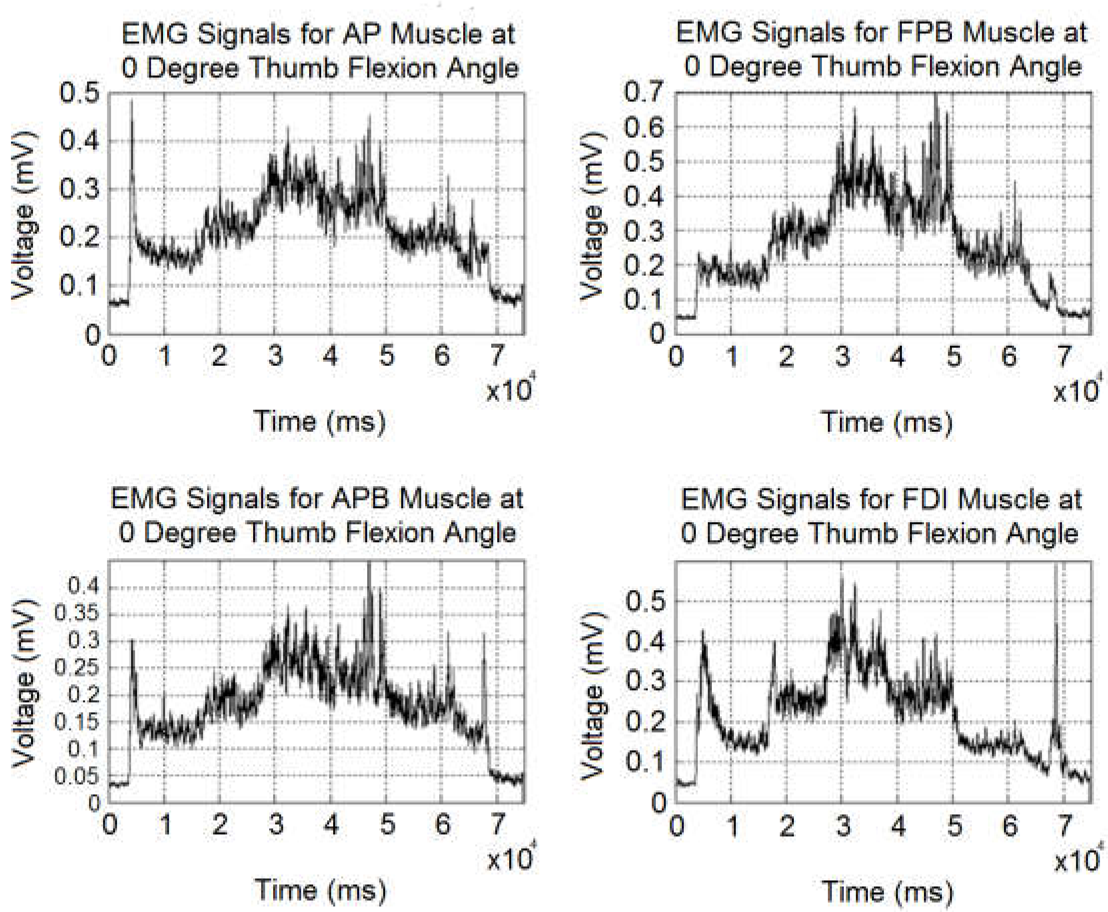


Figure: EMG signals fro different muscles

# 1. Hill's muscle model to predict thumb tip force – muscle length

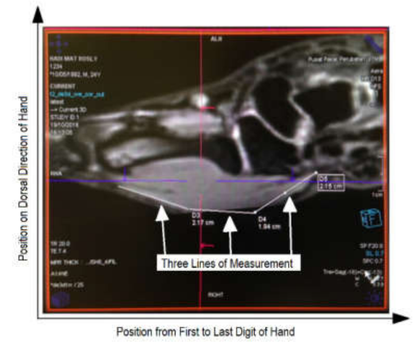


Fig. 8. APB muscle measured by MRI machine

**MRI to provide gold standard**

Figure 3.15: Measuring FDI muscle at 60° flexion angle

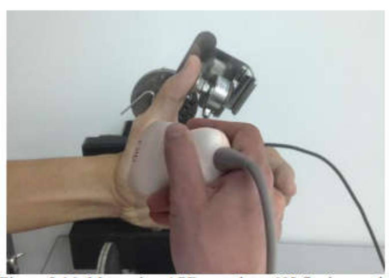

Figure 3.16: Measuring APB muscle at 60° flexion angle

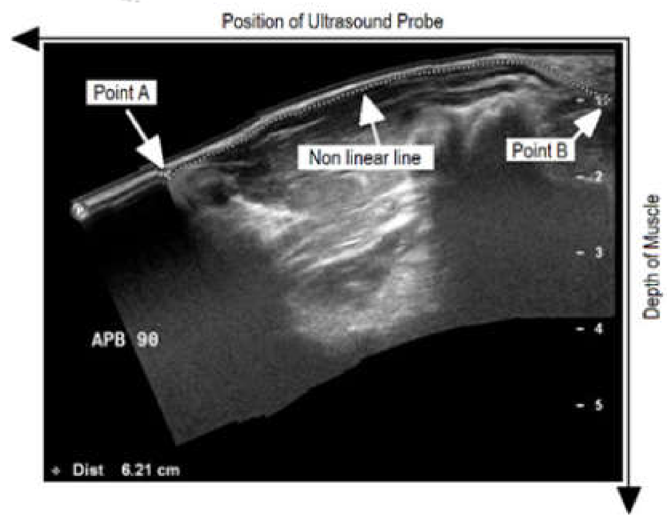


Fig. 9. APB muscle measured by ultrasound probe

Figure: Measurement by ultrasound machine by radiologist

# 1. Hill's muscle model to predict thumb tip force

Table 3. Muscle length measured from MRI and ultrasound (Ult.) signals

| Sub | Muscle | 0° MRI (cm) | 0° Ult. (cm) | 30° Ult. (cm) | 60° Ult. (cm) | 90° MRI (cm) | 90° Ult. (cm) |
|---|---|---|---|---|---|---|---|
| Sub. 1 | AP | 3.51 | 3.52 | 4.31 | 5.64 | 5.93 | 5.93 |
| | FPB | 4.76 | 4.72 | 5.17 | 5.39 | 5.60 | 5.60 |
| | APB | 4.75 | 4.75 | 5.37 | 5.83 | 6.09 | 6.02 |
| | FDI | 6.37 | 6.33 | 6.46 | 6.63 | 6.92 | 6.96 |
| Sub. 2 | AP | 3.14 | 3.08 | 4.24 | 4.61 | 5.64 | 5.63 |
| | FPB | 4.86 | 4.81 | 4.93 | 5.13 | 5.31 | 5.25 |
| | APB | 5.96 | 5.64 | 5.81 | 6.02 | 7.00 | 6.36 |
| | FDI | 5.17 | 5.24 | 5.34 | 5.44 | 5.69 | 5.66 |
| Sub 3 | AP | 3.43 | 3.41 | 3.88 | 4.65 | 5.07 | 5.06 |
| | FPB | 4.65 | 4.55 | 4.83 | 5.12 | 5.60 | 5.57 |
| | APB | 5.3 | 5.29 | 5.43 | 5.93 | 6.26 | 6.21 |
| | FDI | 5.07 | 5.08 | 5.35 | 5.68 | 6.46 | 6.01 |

Table 4. Optimised values of $F_{CE_{max}}$, $L_{CE_0}$, $\emptyset$, $S$ and $A$

| **Muscle** | $F_{CE_{max}}$ **(N)** | $L_{CE_0}$ **(cm)** | $\emptyset$ | $S$ | $A$ |
|---|---|---|---|---|---|
| AP | 260.281 | 5.366 | 0.723 | 0.010 | 0.724 |
| FPB | 207.790 | 4.993 | | | |
| APB | 92.289 | 4.363 | | | |
| FDI | 28.009 | 7.040 | | | |

# 1. Hill's muscle model to predict thumb tip force

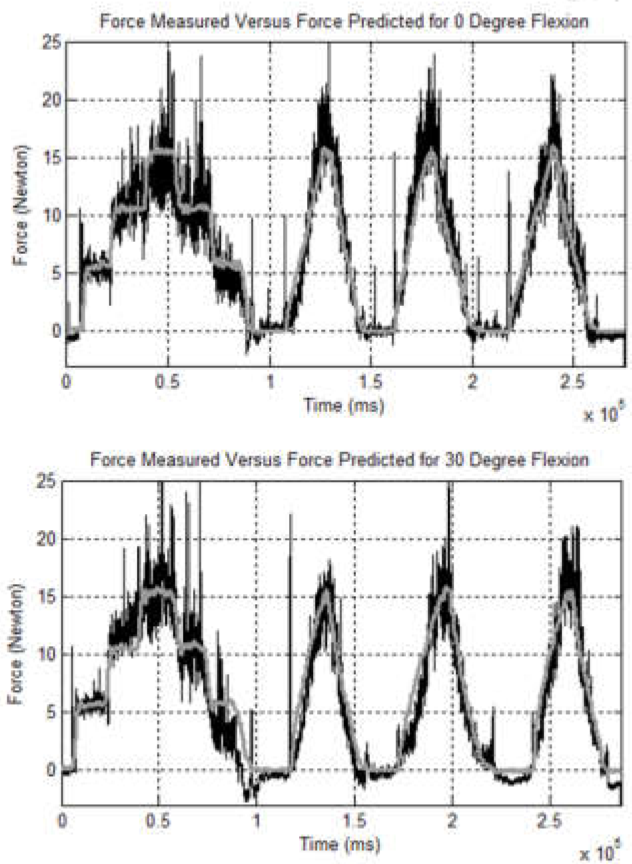


Fig. 11(a). Plot of measured (black) vs. predicted (grey) thumb-tip force at 0° and 30° with new multiplier.

Table 5. RMSE performance of model developed as compared to model by Park et al.

| Flexion angle | Model developed | Park et al., 2012 |
|---|---|---|
| 0° | 1.784 | 1.866 |
| 15° | - | 3.299 |
| 30° | 1.862 | 3.453 |
| 45° | - | 4.425 |
| 60° | 1.822 | - |
| 90° | 1.349 | - |

**More subjects for more universal model**

# 2. Thermal imprint to predict affective states

Explicit and implicit communication plays significant role in effective interaction

- Verbal, facial expression, body language could be emotionally masked causing deterred interaction

Motivation is to leverage autonomic nervous system (ANS) parameters to detect true affective state – used by autonomous agents for effective interaction

# 2. Thermal imprint to predict affective states

Objective: To develop non-invasive, contactless, seamless (subject & sensor) system to identify affective states of subjects from **frontal facial thermal imprint as biosignal**

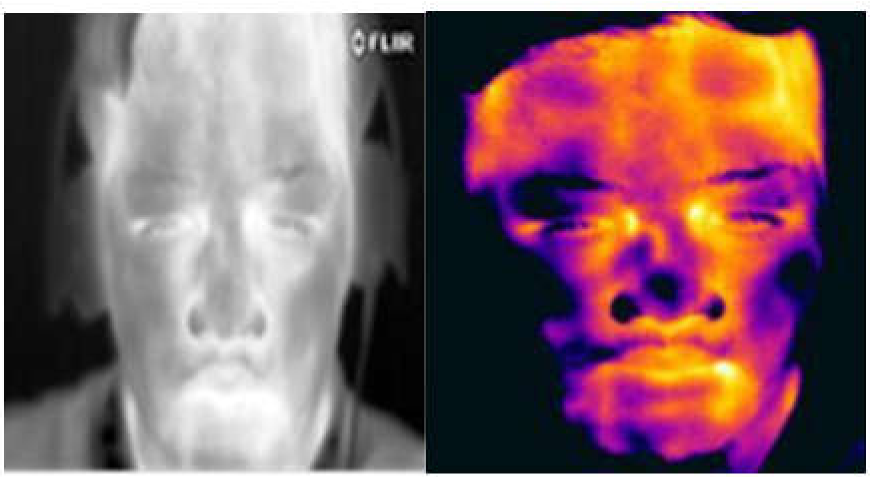


Figure: Sample of thermal image

# 2. Thermal imprint to predict affective states

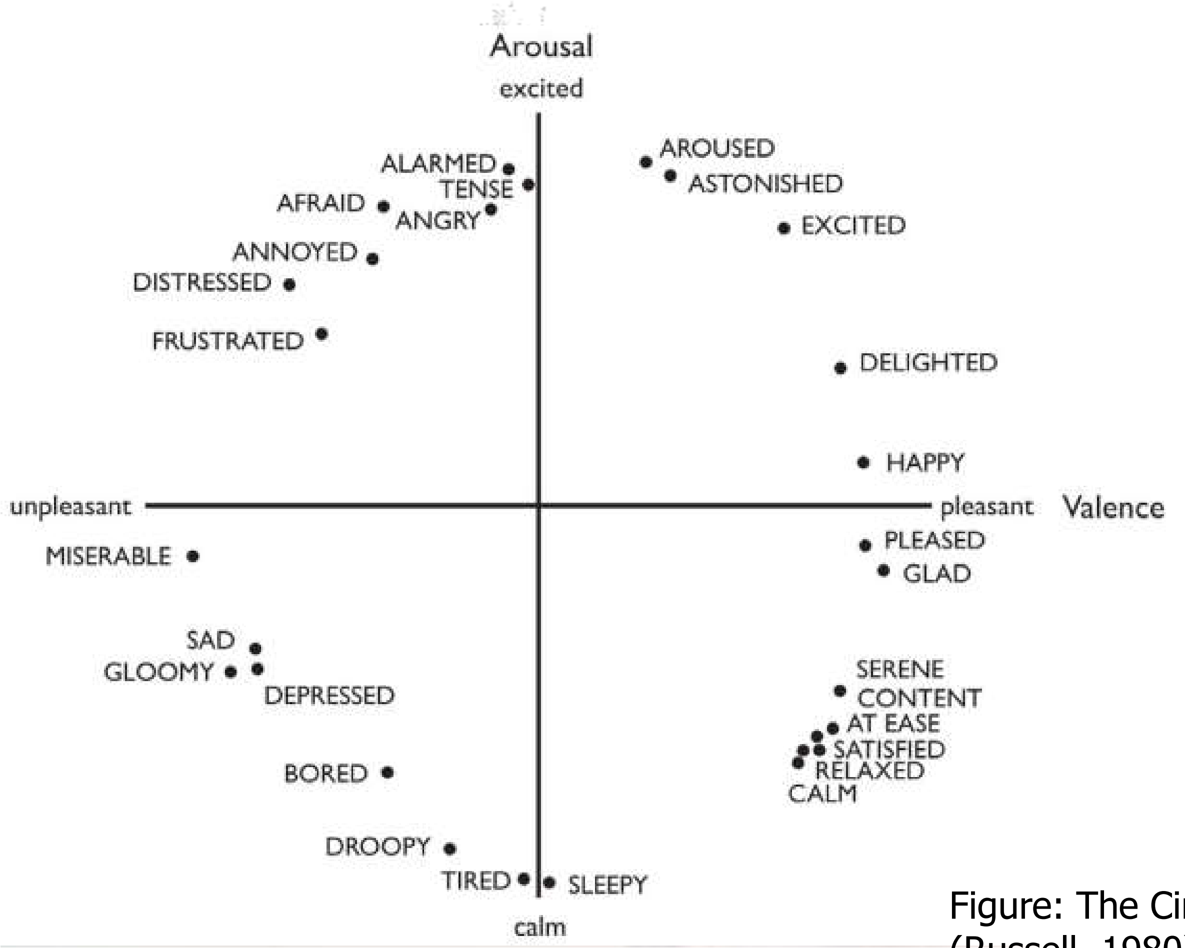


Figure: The Circumplex Model of affect (Russell, 1980) – three principal dimension

# 2. Thermal imprint to predict affective states

| State | Definition |
|---|---|
| Happiness | Feeling of pleasure, satisfaction with performance |
| Fear | Extreme worries, anxiety and panic |
| Anger | Extreme degree of negative affect toward someone or something |
| Disgust | Revulsion, disapproval, annoyance or irritation |
| Sadness | Feeling of melancholy beyond negative self-efficacy |
| Surprise | An unexpected or astonishing event, fact or thing |

Figure: Prototypical emotion (Ekman, 1992) – categorical based classification

# 2. Thermal imprint to predict affective states - methodology

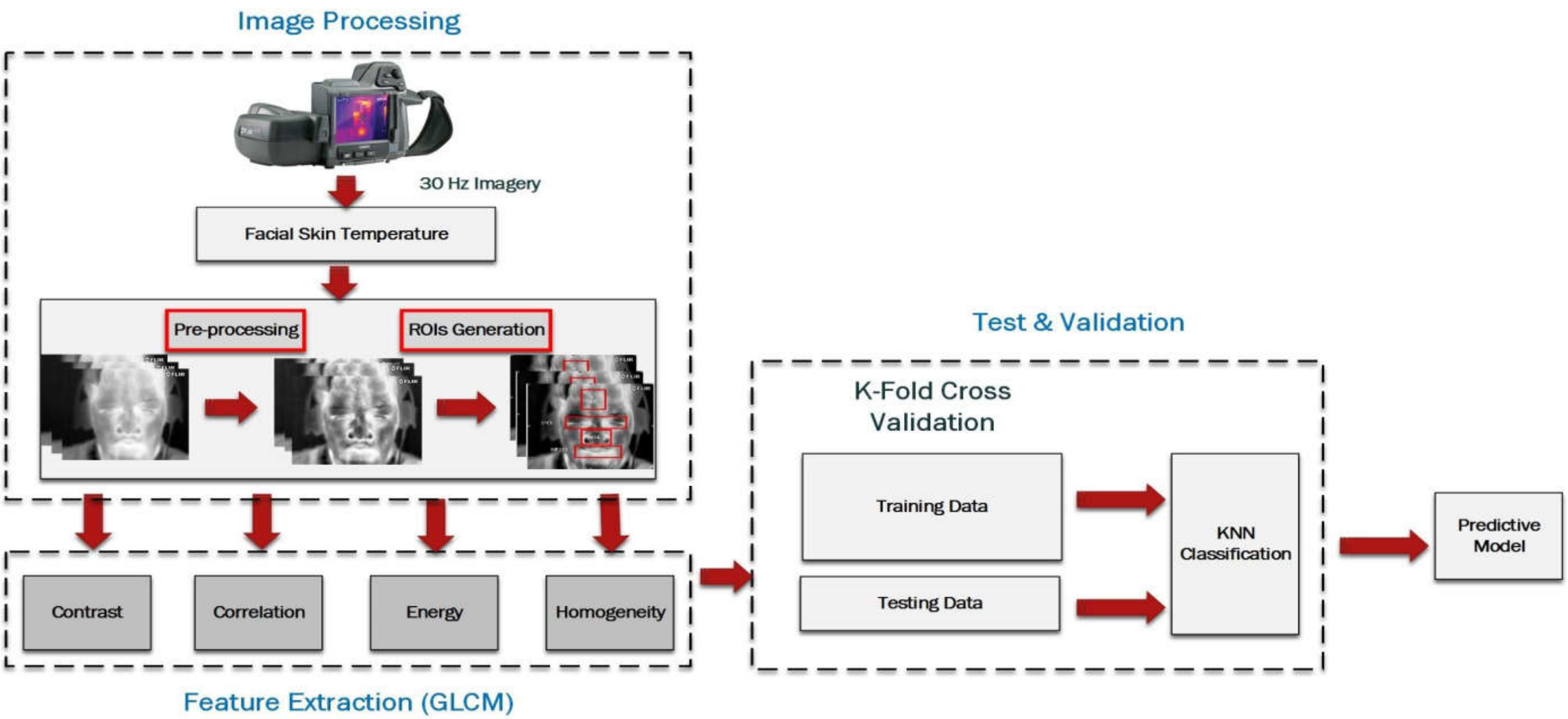


Figure: Framework for affective state identification

# 2. Thermal imprint to predict affective states – experimental setup and procedure

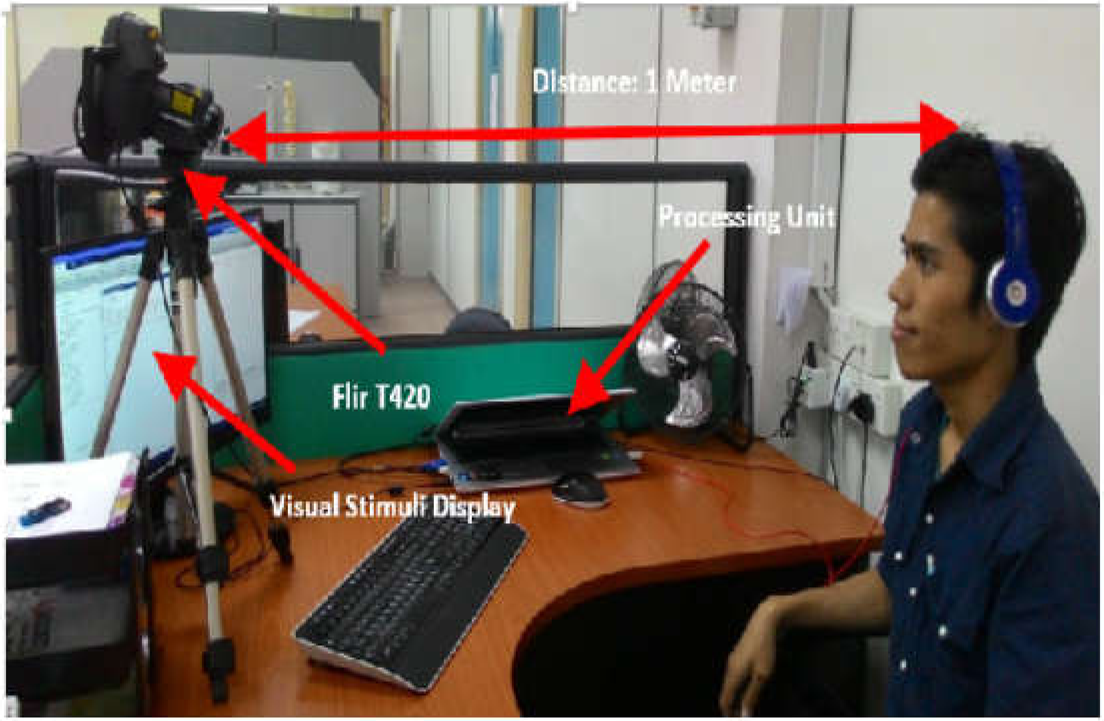


Figure: Experimental setup. Procedure and Questionnaire

# 2. Thermal imprint to predict affective states

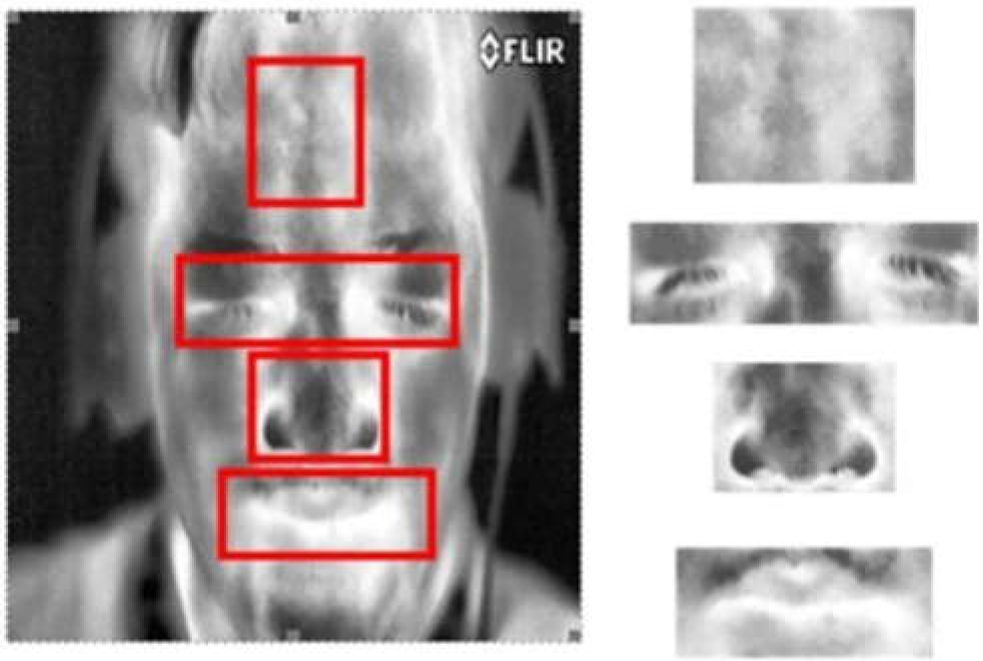


Figure: ROIs: Supraorbital, periorbital, nose and mouth

Feature extracted: Using statistical Gray Level Co-occurrence Matrix (GLCM) :
4-second order statistical features of the image (**contrast, correlation, energy and homogeneity**)

# 2. Thermal imprint to predict affective states

Experiment conducted:
30 healthy subjects, 15 males and female
Age: between 21 to 28 years old
Stimuli: Video clips
The collected data were down sampled to 80 thermal images (from 1200 images) per subject per emotion

Table 4.5: Contribution of Indi

| Interpixel Distance (d) | |
|---|---|
| Feature | d=1 ( |
| CON | 83.8 |
| COR | 88.8 |
| ENR | 79.8 |
| HMS | 80.6 |

Figure: The best result

Table 4.7: The Accuracy of Two Combined Features

| Interpixel Distance (d) | | |
|---|---|---|
| Feature | d=1 (Accuracy) | d=2 (Accuracy) |
| CON | 83.8% (+) | 83.5% (+) |
| COR | 88.8% (+) | 89.3% (+) |
| ENR | 79.8% (-) | 77.3% (-) |
| HMS | 80.6% (-) | 79.4% (-) |
| Average | 83.25% | 82.38% |
| CON-COR | 86.6% | 86.5% |

# 2. Thermal imprint to predict affective states

Table: Confusion Matrix for 6 basic emotions

| Predicted Class | | | | | | | |
|---|---|---|---|---|---|---|---|
| Actual Class | | Disgust | Angry | Fear | Happy | Sad | Surprise |
| | Disgust | 30553 (79.6%) | 1755 | 1257 | 1171 | 2225 | 1439 |
| | Angry | 1158 | 34142 (88.9) | 605 | 693 | 1045 | 757 |
| | Fear | 887 | 582 | 34636 (90.2) | 710 | 996 | 589 |
| | Happy | 670 | 574 | 528 | 35497 (92.4) | 614 | 517 |
| | Sad | 2123 | 1722 | 1310 | 1059 | 30947 (80.6) | 1239 |
| | Surprise | 1132 | 877 | 717 | 733 | 991 | 33950 (88.4) |

**Performance: Average classification accuracy of 86.7%.**

# 2. Thermal imprint to predict affective states - children

Figure: Experimental setup

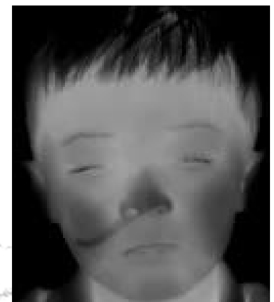

Figure: Image from Flir T420

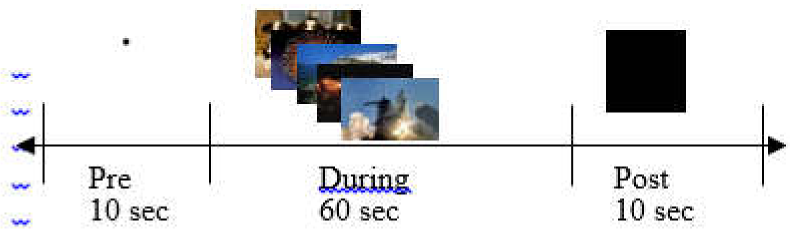


Figure: Timeline for stimuli

# 2. Thermal imprint to predict affective states

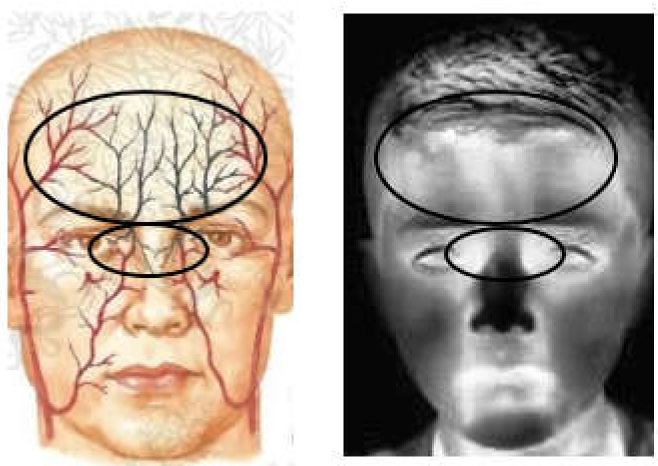

Figure: ROIs: Supraorbital, periorbital

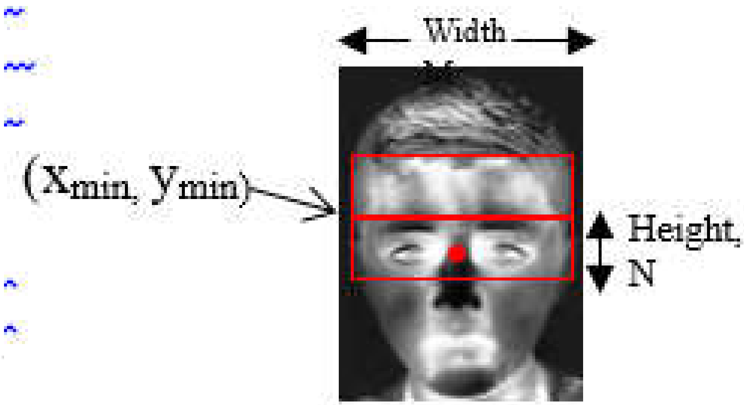


Feature extracted:
**Average intensity values**
**Area of blood vessels**

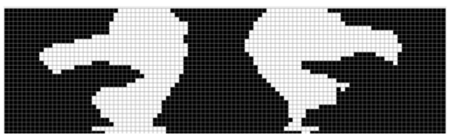

From GLCM :
**Contrast**
**Correlation**
**Dissimilarity**

# 2. Thermal imprint to predict affective states

Experiment conducted:
16 healthy subjects,
Age: between 6 to 9 years old
Stimuli: Pictures from IAPS – In
The collected data were down s
images) per subject per emotior
Sad is not considered due to lov

| ROI | Affective States | j=1 | j=2 | j=3 |
|---|---|---|---|---|
| SupraOrbital | Angry | 0.91 | 0.86 | 0.78 |
| | Disgust | 0.9 | 0.85 | 0.77 |
| | Fear | 0.91 | 0.85 | 0.78 |
| | Happy | 0.91 | 0.86 | 0.78 |
| | Surprise | 0.9 | 0.85 | 0.77 |
| PeriOrbital | Angry | 0.9 | 0.85 | 0.77 |
| | Disgust | 0.89 | 0.84 | 0.76 |
| | Fear | 0.9 | 0.85 | 0.77 |
| | Happy | 0.88 | 0.84 | 0.76 |
| | Surprise | 0.9 | 0.85 | 0.77 |

Different threshold values from MOC

# 2. Thermal imprint to predict affective states

| (Region of Interests (ROI) | Hottest region threshold value | Performance of accuracy (%) (correctly classified) k-NN classifiers |
|---|---|---|
| **Supraorbital** | At 50% | 89.9 |
| | At 90% | 92.4 |
| | At MOC of j=1 | 92.4 |
| | At MOC of j=2 | 84.8 |
| | At MOC of j=3 | 91.1 |
| **Preorbital** | At 50% | 94.9 |
| | At 90% | 93.7 |
| | At MOC of j=1 | 88.6 |
| | At MOC of j=2 | 93.7 |
| | At MOC of j=3 | 96.2 |
| **Combined ROIs (Supraorbital + Preorbital)** | At 50% | 97.5 |
| | At 90% | 98.7 |
| | At MOC of j=1 | 97.5 |
| | At MOC of j=2 | 93.7 |
| | At MOC of j=3 | 99.2 |

# 2. Thermal imprint to predict affective states

Ongoing study on Small Children with Autistic Spectrum Disorder (ASD) to solve <u>the problem of social interaction difficulties</u>

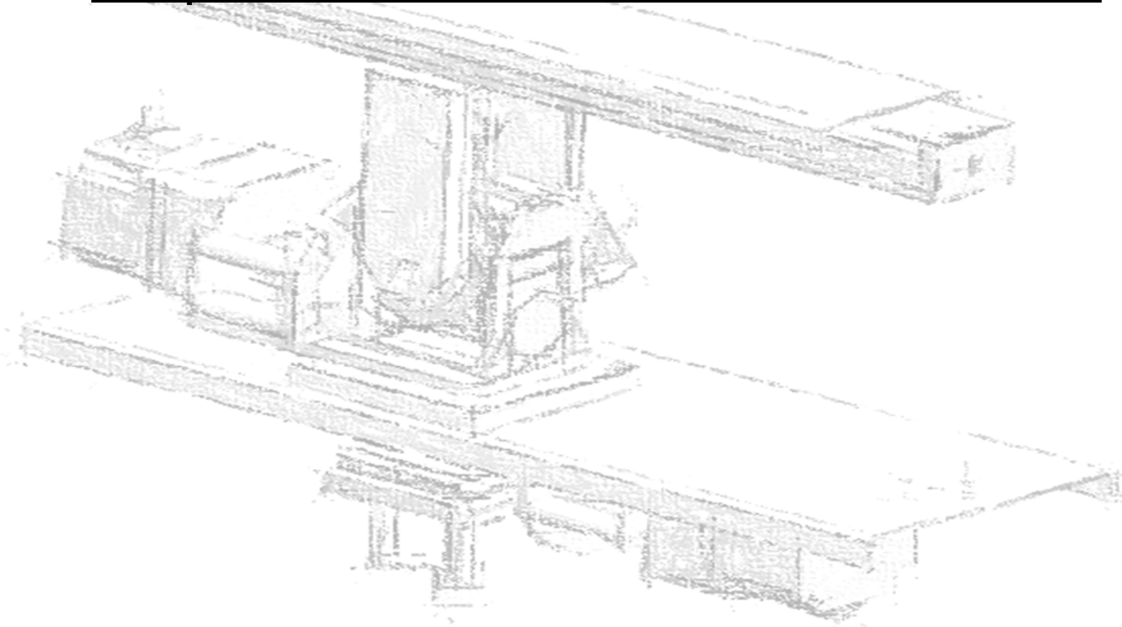

# The End

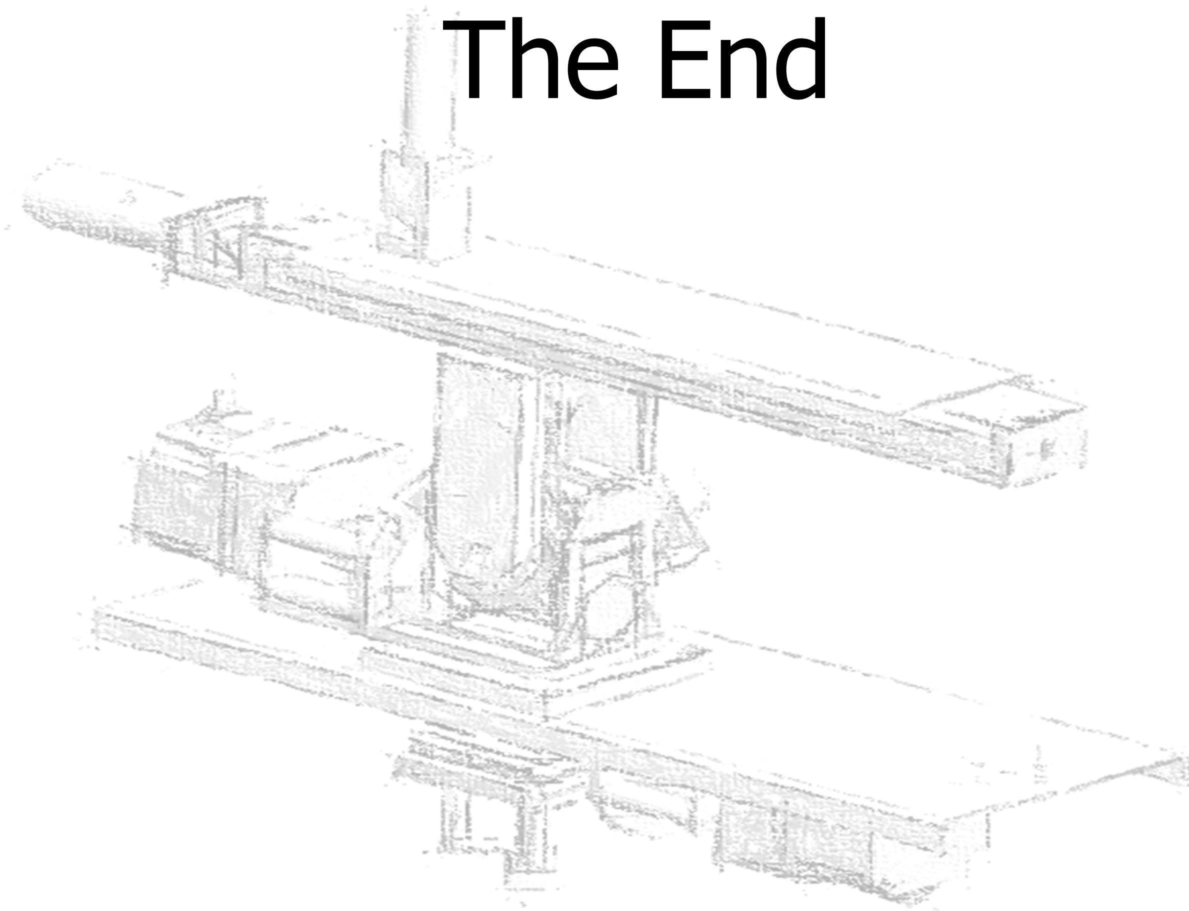

Reference:

1. Biomedical Signals and Sensors I, DOI : 10.1007/978-3-642-24843-6_1